Towards Early Warning for Damages to Cultural Heritage Sites: The Case of Palmyra

Daniele Cerra and Simon Plank

Abstract The intentional damage to local cultural heritage sites carried out in recent months by the Islamic State has received wide coverage from the media worldwide, raising the awareness for the need of prompt, safe, non-invasive damage detection and assessment surveys. Earth observation data represents the only reliable, non-invasive information source in areas which are not accessible due to conflicts or natural disasters. In order to provide a fast response, automated image processing techniques are needed to speed up the analysis. This chapter shows a comprehensive case of study for damage detection and monitoring in time through a series of satellite images acquired over the city of Palmyra, Syria, which suffered huge losses related to its cultural heritage in a time span longer than a year. Maps highlighting potential damages are derived from robust change detection techniques, based on changes in the textural features characterizing pre- and post-disaster satellite data. Such information could help experts at timely assessing the damages to cultural heritage sites of interest, and a chronological study of the different damages can be produced if a satellite image time series is available on the site of interest. Furthermore, the idea of marking sensitive areas characterized by different criticality is introduced: early damage detection routines could thus be restricted to the most important or threatened sites or expanded to larger areas or surrounding urbanizations. For this purpose, a pair of images acquired on the city of Sirwah, Yemen, are analysed, and the change detection results are discussed in this frame.

Keywords Cultural heritage · Palmyra · Earth observation monitoring · Change detection techniques · Damage assessment

D. Cerra (✉) · S. Plank
Earth Observation Center (EOC), German Aerospace Center (DLR), Münchner str. 20, Weßling, Germany
e-mail: Daniele.Cerra@dlr.de

D. G. Hadjimitsis et al. (eds.), *Remote Sensing for Archaeology and Cultural Landscapes*, Springer Remote Sensing/Photogrammetry,
https://doi.org/10.1007/978-3-030-10979-0_13

Introduction

When the Islamic State (IS) was rumoured in the media to have destroyed cultural heritage (CH) sites in Syria—in particular in the city of Palmyra—the sites of interest were inaccessible to any legal authority in order to confirm the damage through an in situ visual inspection by traditional means. Therefore, the Orient Department of the German Archaeological Institute (DAI) tasked the experts of the remote sensing department of the German Aerospace Center (DLR) to assess any damage using high-resolution satellite data. A visual analysis confirmed the destructions claimed by the IS, confirming damages to the Temple of Bel and several tower tombs within Palmyra's ancient necropolis (Plank et al. 2015). The availability of high-resolution satellite images is steadily increasing, along with their quality and temporal resolution. Remote sensing is therefore capable of providing the only non-invasive way of observing and recording changes in the archaeological landscape for conflict areas and inaccessible sites (Lasaponara and Masini 2011).

If several images of the same site are available, of which at least one acquired before a given event and one afterwards, a change detection analysis can be carried out to assess the damages caused by a natural disaster or as a consequence of human conflicts. Usually such task is performed by visually verifying the integrity of critical sites and relevant infrastructures in the area of interest. Whenever the affected area is large and a rapid response is desired, however, this manual approach presents several drawbacks. On the one hand, it becomes a difficult and time-consuming activity; on the other hand, damaged areas could remain undetected for an observer, if the time available for the analysis is limited. Therefore, an approach with a certain degree of automation would be preferable.

Automatic analysis of Earth observation (EO) data has been successfully employed for several archaeological applications, especially the systematic detection of CH sites. In Lasaponara and Masini (2007), pan-sharpened multispectral QuickBird (DigitalGlobe, Westminster, CO, USA) images are exploited to detect crop marks related to buried archaeological remains. An image-based methodology for the detection of archaeological buried relics using multi-temporal satellite imagery was derived in Agapiou et al. (2013) observing the phenological cycle of the crops. Automatic detection of ancient Arabian tombs through high-resolution satellite imagery was proposed in Schuetter et al. (2013), while an automatic detection of ancient circular structures based on VHR QuickBird images in Southeast Norway has been described in Trier et al. (2009). Recently, previously undocumented cities in Cambodia have been mapped beneath vegetation using airborne LIDAR (Evans 2016). Monitoring and risk assessment of CH sites at landscape scale have been proposed in Agapiou et al. (2016) by integrating a variety of satellite sensors bearing different spatial and spectral resolutions, using geographic information systems (GIS) to cluster cultural heritage sites and monuments with similar characteristics.

Although automatic methods are often used as in the examples listed above, damage detection to CH sites is usually carried out by visual analysis: see Casana and Panahipour (2014) for an example in Syria or other cases of study in Contreras (2010) and Cunliffe (2014). In Lasaponara and Masini (2012), the need of expanding

automatic or semi-automatic procedures to a wider range of archaeological applications is discussed.

In this chapter we apply a change detection algorithm based on differences of textural features in order to go towards the automatic production of maps where areas suspected of having suffered damages are highlighted.

Results are based on robust differences of texture features, yielding reliable change maps with a certain tolerance to co-registration errors and geometric distortions caused by different acquisition angles. The map contains a potential set of sensitive areas on which a more detailed analysis should be carried out by the experts.

The change detection workflow has been tested on images acquired in Palmyra in Cerra et al. (2016). In the present work, two additional images are added to the set of the three available acquisitions previously processed. The different change detection maps are merged in order to successfully visualize the evolution in time of the detected damages in the area and validated against official reports.

An automatic or semi-automatic early warning system would ideally work as follows: at first, sensitive areas containing endangered CH sites should be selected; subsequently, whenever a new acquisition from an optical satellite is available, an automatic change detection procedure would take place. If a relevant change is detected within any area of interest, an alert would be raised and analysed by an operator, who in the end will determine if the change could really correspond to damage to the site.

In periods of war, civil unrest, political instability or after a natural disaster, the sensitivity of a given area could change. Therefore, we analyse a second case of study in Sirwah, Yemen, to introduce the possibility of a configurable selection of sensitive areas with different priority. The user can select beforehand larger areas in which it would be of interest to receive alerts on newly produced damages, but only if one of the aforementioned cases arise. In this case, areas with lower priority such as urbanizations in the immediate proximities of the CH sites and infrastructures would be added to the sites under observation. Once it becomes necessary to increase the attention in an area of interest, this would be done immediately using the preselected areas, increasing the timeliness of the analysis and facilitating a quick response.

The paper is structured as follows. Section "Change Detection Based on Textural Differences" describes the features used to carry out the damage detection. Results of multi-temporal analysis on the archaeological sites of Palmyra are described in section "Case Study: Palmyra", while section "Damage Detection: 2015" proposes a possible configurable early warning system for damage detection to CH sites. We conclude in section "Conclusions".

Change Detection Based on Textural Differences

Change detection aims at providing a map of changes given as input two or more images acquired at different times over the same area. For the applications described in this chapter, the desired output should highlight the locations of monuments that

suffered damage or changes in the time span between the two acquisitions. Automatic change detection techniques may be difficult to apply in practice. For example, the differences between pre- and post-event images may be difficult to obtain in a reliable way if the acquisition dates of the two images are too far away. Even if this is not the case, a pixel-based analysis is difficult to carry out even after an accurate co-registration step, as often no high-resolution digital surface model (DSM) is available. In this case, images may exhibit orthorectification errors, and the differences in view angle introduce, in turn, pronounced geometric distortions.

Gabor features are robust to two-dimensional shifts in space and are traditionally employed in edge detection and edge characterization tasks (Manjunath and Ma 1996). They can be described as a windowed Fourier analysis, compensating for the lack of spatial dependency of features in the frequency domain. They are therefore able to capture the interactions between neighbouring pixels in a local window by quantifying the roughness or smoothness in a specific point, along with its scale and orientation. A bank of Gabor filters usually consists of a set of complex linear filters encompassing the characteristics that stand out for the human eye and agreeing well with how the human visual system's 2D receptive fieldworks (Grigorescu et al. 2002). Each element in the filter bank is derived by transforming in time domain two-dimensional impulses in the frequency domain and multiplying the result by a Gaussian function, which acts as an envelope. In Fig. 1 different orientations and scales of the two-dimensional waves are reported, with the envelope being the weighting function suppressing the response of the filter as a function of the distance from its centre. The higher the frequency of the captured texture, the smaller the envelope can be. Therefore, each component in the filter bank can be defined in its discrete form by varying the frequency f and the orientation θ of the plane waves as proportional to:

$$G_c[k,l] = e^{-\frac{k^2+l^2}{2\sigma^2}} \cos\left(2\pi f\left(k\cos\theta + l\sin\theta\right)\right), \tag{1}$$

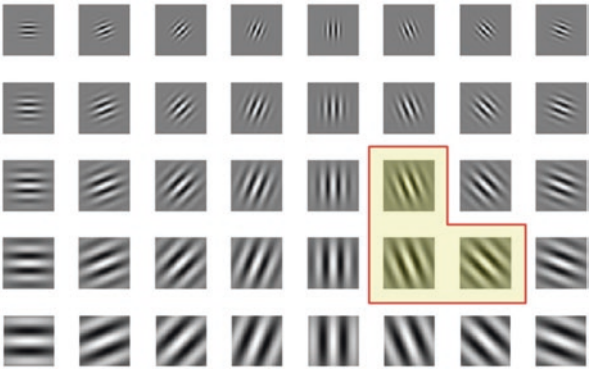

Fig. 1 Real parts of the Gabor filter bank used in the experiments in this paper according to the different orientations and scales. Highlighted are the filters giving the highest contribution to the detection to be described in the next section

$$G_s[k,l] = e^{-\frac{k^2+l^2}{2\sigma^2}} \sin\left(2\pi f\left(k\cos\theta + l\sin\theta\right)\right), \tag{2}$$

where k and l are the extension in number of pixels of the filter, usually with $k = l$, and σ^2 the variance of the Gaussian function used to define the envelope: the smaller the σ, the smaller the effective area in which a specific texture detector for one orientation and scale is applied. An example for the real parts of the filter bank used in the experiments contained in this paper is reported in Fig. 1. Before their application, the filters should be multiplied by a normalization factor chosen in order to have the sum of the responses of the filter to the same sinusoidal function as 1 (Ramakrishnan et al. 2002). The filter banks in Eqs. (1) and (2) are convolved with the image to generate the response centred at each pixel as R_c and R_s. The final value for the response of a pixel to a specific filter in the filter bank is then computed as:

$$B[i,j] = \sqrt{R_c[i,j]^2 + R_s[i,j]^2}. \tag{3}$$

This value is proportional to the similarity of the observed area with the grey-value distribution for a given frequency and orientation in the filter bank. Some generic experiments on damage detection using Gabor features have been carried out in Vijayaraj et al. (2008). In our case, for two co-registered images acquired at $t1$ and $t2$, the difference in texture for an image element at location (i, j) for a given frequency f, rotation θ and spread σ is quantified as:

$$D_G(i,j) = abs\left(R_{t1}[i,j] - R_{t2}[i,j]\right). \tag{4}$$

R_{t1} $[i, j]$ and R_{t2} $[i, j]$ are the results of independently applying Eq. (3) to the same image element in the two images.

To produce a final binary change map, all pixels with textural difference larger than a selected threshold can be selected. Morphological filtering (opening and closing) is subsequently applied to the binary thresholded image to produce the final results.

Case Study: Palmyra

We analysed the archaeological site of Palmyra in Syria, which has been reported to have suffered damage from terrorist activities from 2015 to the beginning of 2017, and the case of Sirwah in Yemen. The latter will inspire a configurable selection for sensitive areas to be monitored with different priority. The locations of these two sites are reported in Fig. 2.

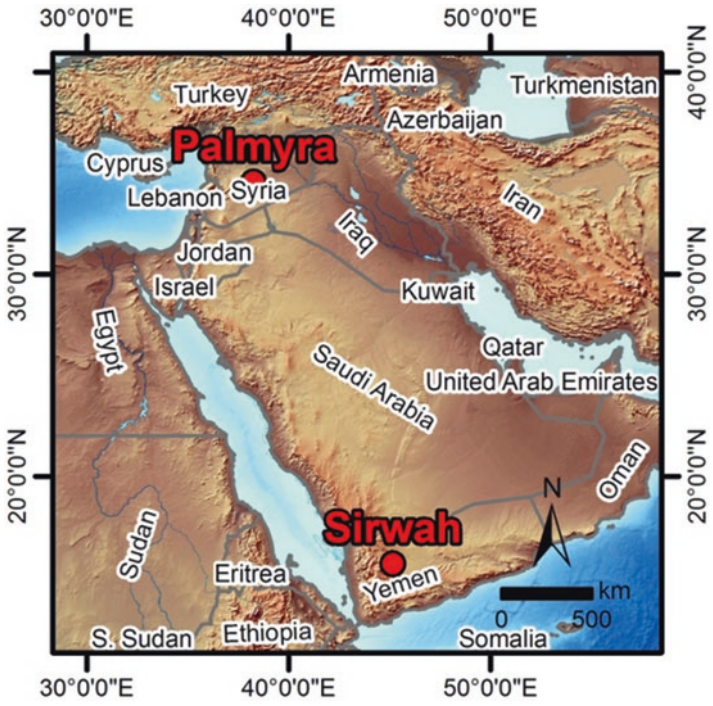

Fig. 2 Map showing the locations of the two sites analysed in this paper

Damage Detection: 2015

Most of the experiments contained in this chapter are carried out on the large archaeological site of Palmyra, situated in the Syrian Desert northeast of Damascus, which have been listed as UNESCO World Heritage site since 1980. One of the most important monuments within the walled city is known as Sanctuary of Bel, on which the first excavation missions took place in the area (Starcky and Munajjed 1960), dedicated to the Gods Bel, Iarhibol and Aglibol in the first century A.D. (Cantineau 1934). The Temple dedicated to the Semitic God Bel (Fig. 3a), whose worship was dominant in the Palmyrene religious cult (Danti 2001), is located in the centre of the Sanctuary. It dates back to the Hellenistic period and received several architectural modifications throughout the first two centuries A.D., which make it of great importance according to scholars for its rich and diverse architectural details (Cantineau 1934; Danti 2001). Sadly, the Temple of Bel became famous on a planetary scale for being among the CH sites in the area to have suffered the worst damage from terrorist activities perpetrated by the IS.

Important vestiges of rich Palmyra's cultural heritage are to be found outside the walls of the city. The western part of Palmyra's ancient necropolis contains what are known as tower tombs (Fig. 3b), erected during the first and second centuries A.D.,

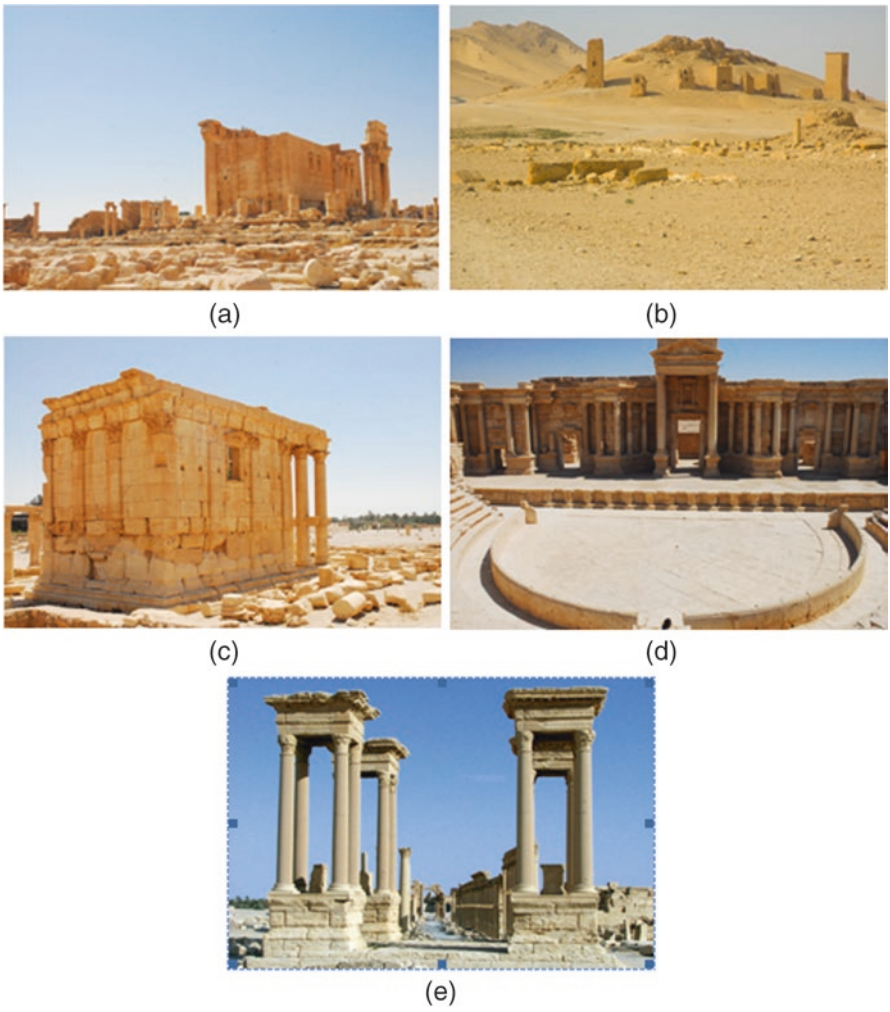

Fig. 3 Palmyra's archaeological sites discussed in this work: (**a**) Temple of Bel @ Michael Danti; (**b**) tower tombs in the background @ szymanskim; (**c**) Temple of Baalshamin @ Michael Danti; (**d**) Roman theatre @ Michael Danti; (**e**) tetrapylon @ DGAM

which contained burial items, decorations and wall paintings representing an important source of information related to the cultural habits of the ruling class of the city. The tower tombs underwent severe damages in the last years, part of which will be analysed in the next section.

Other important monuments (Bryce 2014) include the Temple of Baalshamin, dating back to the second century B.C. (Fig. 3c), a Roman theatre founded in the second century A.D. (Fig. 3d), and the tetrapylon, a cubic monument with four gates usually placed on important crossroads (Fig. 3e).

Fig. 4 Subset of the WorldView-2 image acquired on the 27th of August 2015 (European Space Imaging/DigitalGlobe)

Fig. 5 Subset of the WorldView-2 image acquired on the 2nd of September 2015 (European Space Imaging/DigitalGlobe)

Figures 4 and 5 report the subsets of two WorldView-2 datasets acquired outside the city centre of Palmyra on the 27th of August and on the 2nd of September 2015, dates that henceforth we denote with $t1$ and $t2$, respectively. At time $t1$, the IS had already destroyed several CH sites in the area, such as the Temple of Baalshamin. This loss must be added to the huge number of artefacts destroyed or illegally sold to finance IS activities (ref. the companion book chapter "Recent Destructions in Palmyra/Syria, Looting and Illegal Antiquities Trade"). Between $t1$ and $t2$, other tower tombs and the Temple of Bel were damaged. In the figures, the Temple of Bel is located in the southeast, while the tower tombs are scattered in the north-western part of the image. In our first step, the co-registration of the images has been refined by automatically deriving 1000 Ground Control Points by matching of scale-invariant feature transform (SIFT) features (Lowe 2004) between the two images and by warping the image acquired at time $t1$ using as reference the image acquired at time $t2$.

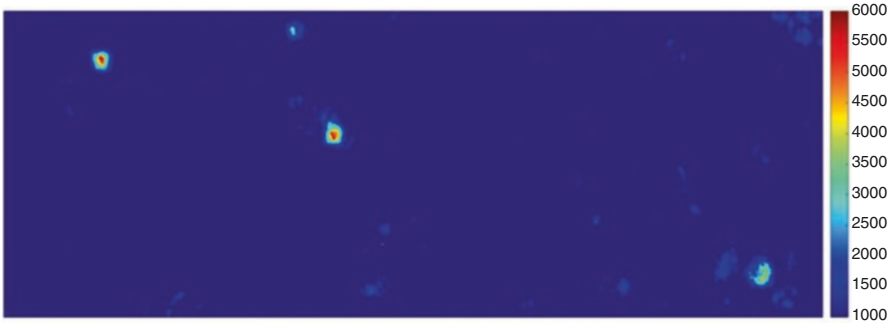

Fig. 6 Change detection map between the two images reported in Figs. 4 and 5. The four targets which stand out clearly represent detected damages to three clusters of tower tombs (upper left) and to the Temple of Bel (lower right)

We employ a standard Gabor filter bank, capturing the texture information in a geometric grid having any combination of 5 different scales with 8 possible orientations, analysed in a window of size 39×39, for a total of 40 filters (Haghighat et al. 2015). Figure 1 reports the real parts of the filters: the most important features for the analysis carried out in the rest of this section are highlighted and are related to the scale of the objects of interest and the shadow orientation, dependent on the sun's elevation angle.

As textural features are usually computed on a single spectral band, we choose in all cases the red band as it haves a high quality for the WorldView sensors which is independent from the off-nadir acquisition angle (Aguilar et al. 2013).

To derive a change map, also the brightness information is taken into account in this case, and brightness robust difference (RD) features (Tian et al. 2014) are computed using a window of size 9×9, which was found to give more robust results. As the contribution to the change map of RD was smaller than the robust texture differences, we did not compute RD in the experiments reported in the next sections.

The overall change map in Fig. 6 is produced by normalizing and averaging the textural and brightness differences. If a binary map showing the locations of possible damages is desired, the final changes are highlighted from a manually thresholded version of the change map, after applying a single pass of morphological opening and closing. The structuring element of choice for the morphological filter was a disc of size 3, corresponding to a 3×3 square window filled with ones, with zeros in the four corners.

The binary map is overlaid on the image acquired over Palmyra at time $t2$ in Fig. 7.

The map indicates the destruction between $t1$ and $t2$ of several tower tombs and of the central part of the Temple of Bel on the right of Fig. 7. The validation of these changes will be discussed at the end of this section: to have a complete frame, it is of interest to consider also the additional damages to cultural heritage sites in the area which had been carried out before $t1$, time for which we have our first available image.

Fig. 7 Red: Post-processed change map from Fig. 6 overlaid on the 2nd of September 2015 WorldView-2 image reported in Fig. 5. All the main damaged areas are correctly identified (European Space Imaging/DigitalGlobe)

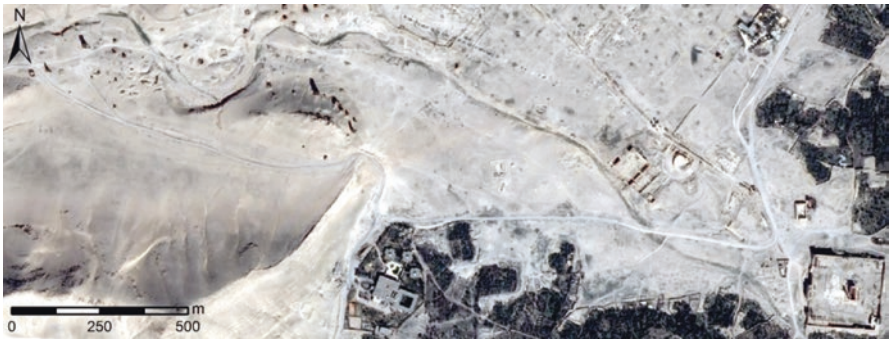

Fig. 8 Pre-disaster image acquired on the 20th of February 2014, screenshot from Google Earth (DigitalGlobe)

In order to ideally travel back in time, we extracted an image available on Google Earth (version 7.1.5.1557, Google Inc., Mountain View, CA, USA) which was acquired on the 20th of February 2014. We refer to this date as time $t0$. The image reported in Fig. 8 shows all relevant monuments still intact.

In this and the next experiments, only textural differences have been considered: on the one hand, they proved to be the most meaningful and robust; on the other hand, blending together the results obtained through textural and brightness robust differences requires the tuning of additional parameters which should be ideally skipped, if a certain degree of automation is desired in the workflow. The image extracted from Google Earth is co-registered to the image acquired at time $t2$, and differences based on Gabor features are computed in the same way as in the previous experiment. The final results are reported in Fig. 9. All the relevant damaged areas are detected, including the Temple of Bel and the tower tombs: the most meaningful result is represented by the additional detections which correctly correspond to the Temple of Baalshamin (in the north-eastern part of the image), the tombs of

Fig. 9 Red: post-processed changes overlaid on the 2nd of September 2015 WorldView-2 image reported in Fig. 5. All the main damaged areas are correctly identified with two small false alarms in the southern part of the image (European Space Imaging/DigitalGlobe)

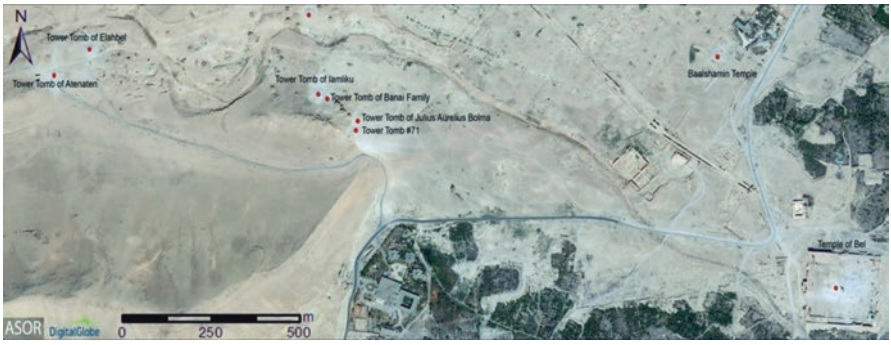

Fig. 10 Report from Cuneo et al. (2015) showing destroyed CH sites in Palmyra. This map was used as validation for the detected damaged areas (ASOR CHI/DigitalGlobe)

Iamliku with the tomb of the Banai family directly to its east (merged in a single area in the centre-left of the image) and the tomb of Atenaten (in the northwest). Only two false alarms are visible in the lower central part of the image.

The final damage detection can be validated against a map representing all relevant CH sites destroyed produced by the American School of Oriental Research (ASOR) in the report on the situation in Palmyra (Cuneo et al. 2015) depicted in Fig. 10. According to the report, between $t1$ and $t2$ the following monuments have been destroyed: the Temple of Bel, the tomb of Elahbel, the tomb of Kithoth in the northern part of the necropolis, the tomb of Julius Aurelius Bolma and the tomb #71 near the tomb of Iamliku. The damages carried out between $t0$ and $t1$ affected instead the Temple of Baalshamin and the tombs of Atenaten, Iamliku and the Banai family. All of such damages are correctly detected both in time and space.

It is interesting to consider the correspondence between the most useful Gabor features highlighted in Fig. 1 and the damaged buildings in the image. Regarding the scale, Gabor filters in the filter bank are comparable to the damaged objects.

But also the orientation of the filters plays a key role, as it seems to agree with the sun's position and therefore with the direction of shadows on the ground. Variations in the latter could raise false alarms; therefore, it is recommended whenever available to use for the change detection images acquired by a satellite operating in a heliosynchronous orbit.

Analysis of Recent Damage: 2017

On 20th of January, Syria's Director General of Antiquities and Museums confirmed that the IS had destroyed the tetrapylon and part of the facade of the Roman theatre (Danti et al. 2017). Two images are available over this area: one WorldView-3 and one WorldView-2 multispectral images. The former was acquired on the 26th of December 2016 and the latter on the 10th of January 2017. Henceforth, we refer to the mentioned dates as $t3$ and $t4$, respectively.

The two images were not accurately co-registered, so an additional pre-processing step was needed as texture change detection is robust to small co-registration errors but only up to a certain extent. A procedure based on the extraction of SIFT features was therefore carried out as described in previous section. The texture-based change detection applied to the two images results in the change map overlaid in Fig. 11.

Due to the pronounced differences in acquisition angles, some false alarms are present, but the damages to the tetrapylon are clearly detected. Regarding the theatre, only the changes in the central part are detected over a small area. The changes in the Temple of Bel do not correspond to a new damage, as they are caused by the different shapes of the shadows on the ground in the two images.

A subset of the two images is reported in Fig. 12. The tetrapylon and the Roman theatre, which are to be found, respectively, in the top left and bottom right of each image, are visibly preserved at time $t3$. The severe damages suffered by these two CH sites are clearly shown in the image acquired at time $t4$.

Multi-temporal Analysis

A multi-temporal representation of the systematic destructions affecting the cultural sites of Palmyra can be derived by merging the detected damaged areas between images acquired at times $t0$, $t1$ and $t2$ with the most recent damages detected between times $t3$ and $t4$, representing different time spans with different colours. An example is reported in Fig. 13, in which the older damages are highlighted in blue, subsequent destroyed buildings in red and more recent changes in green.

Such multi-temporal analysis cannot exactly determine the exact date in which damages occurred, but can help in reconstructing the evolution of events in sensitive areas.

Fig. 11 Subset of the WorldView-2 image acquired on the 26th of December 2016 ($t3$). Reported in black and white in the yellow square is a subset of the WorldView-3 image acquired on the 10th of January 2017 ($t4$). Damage that occurred between $t3$ and $t4$ is highlighted in light blue

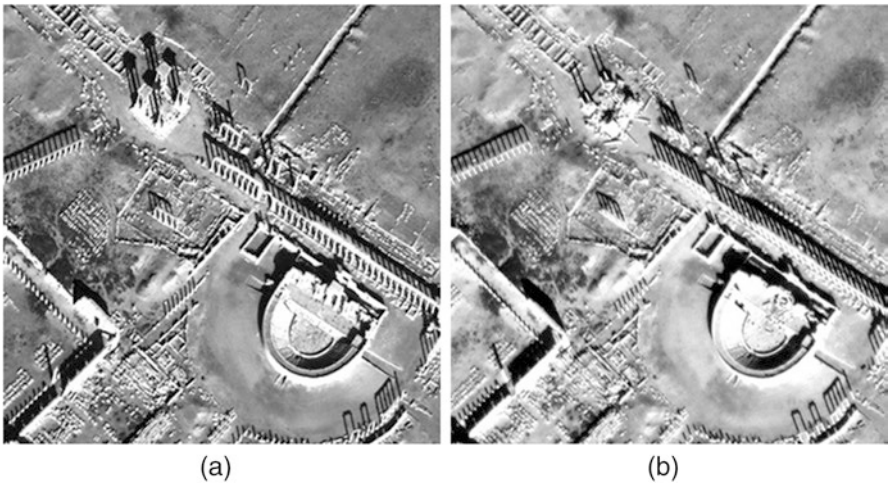

Fig. 12 Detail of image in 11: Theatre (bottom right) and tetrapylon (top left) still intact in an image acquired at time $t3$ (**a**) and appearing destroyed or damaged in an image acquired at time $t4$ (**b**)

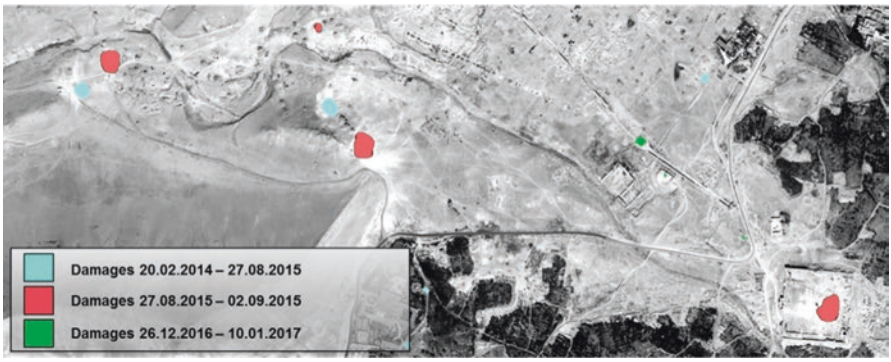

Fig. 13 Multi-temporal representation of damage overlaid on the 2 September 2015 WorldView-2 image reported in Fig. 5 (European Space Imaging/DigitalGlobe). Damage that occurred between $t0$ and $t1$, between $t1$ and $t2$ and between $t3$ and $t4$ is highlighted in blue, red and green, respectively

Setting Up an Early Warning System for Endangered Cultural Heritage Sites

The Sabaean city of Sirwah is located about 40 km to the west of Marib in Eastern Yemen, and it represented the second most important economical and political centre of the Kingdom of Saba in the first century B.C. The historical part of the city comprises several CH sites of particular interest, such as the 780-m-long outer protection wall, the Almaqah temple dating back to the seventh century B.C. and the Athtar temple. Part of these sites has been discovered only recently, with several still ongoing excavations (Gerlach 2017).

In spring 2015 a civil war took place in Yemen, with Sirwah being placed at the frontline between the Houthi rebels and the Arabic alliance supporting the president of the country, making access to the sites difficult and further excavations almost impossible (Al Masdar News 2017). The conservation of Sirwah's CH sites became a concern as air strikes of the Arabic alliance against the Houthi rebels caused massive damages to the modern part of the city, which is located very close to the ancient part, and were assessed by a visual analysis of satellite images before and after the event. This real scenario suggests a possible configuration setting for the monitoring of specific areas rich in CH sites located in sensitive areas.

Whenever human-driven events as in the aforementioned case (e.g. civil war, terrorism) or natural ones (e.g. earthquake, fire, flood) are taking place, it may be of interest to monitor not only the most important CH sites but also the surrounding areas. If the latter would result in damage, the vulnerability of nearby CH sites would probably increase. This leads to the proposed configurable early warning system, in which different priorities could be set to monitor critical areas.

If the ingestion of newly acquired satellite images is constantly being delivered on an area of interest, the user could select the CH sites at risk as areas having maximal

criticality, but also indicate any nearby territory which would need to be monitored in case of dangerous (foreseeable or not) events. Whenever desired, the user could then switch on the monitoring in areas denoted by a lower priority as needed. The negative consequence would be a higher number of raised false alarms not indicating real changes, which should be examined by the user. On the other hand, such analysis would quickly raise awareness on the overall damages, as the areas to analyse would have been set beforehand, speeding up the process.

In the case of Sirwah, comparative analysis of very high-resolution WorldView-2 imagery acquired on the 8th of April 2014 and the 23rd of May 2015 showed no clear changes (possible damages) within the ancient part of the city. However, several damages were detected in the modern area surrounding the CH sites: for instance, the government's palace was completely destroyed. Figure 14 reports a possible definition of areas with different priority in Sirwah and a subset of the comparative analysis results derived from difference in textural Gabor features. On the top of Fig. 14, the area of higher priority containing most of the CH sites of interest in Sirwah is delimited by a red circle denoted by 'CH'. The area around in yellow may represent the surrounding area which it may be desired to monitor in extreme situation, such as the aerial bombings carried out in 2015. If the yellow area would be activated, meaning that it is added to the automatic change detection analysis, the destruction of a building in the modern area of Sirwah would be detected. This is depicted in the lower part of the image, along with the change detection results.

In the case of Palmyra, a possible definition for such areas is reported in Fig. 15. In this example, the main CH sites have been selected for the high priority zone, while a secondary one has been derived by including any object within a 200 m distance from any of the CH sites. Automatic change detection techniques as described in previous sections could be applied only on the high priority zones in absence of ongoing conflicts or to all areas otherwise.

Conclusions

Recent historical events put cultural sites of universal interest under serious threats, with Earth observation data playing an important role in their monitoring, as detailed damage assessment maps are paramount for authorities and stakeholders (Council of Europe 2000). The number of operating spaceborne sensors systems is steadily increasing, along with the imaging capabilities and revisit time of each sensor. The pre-processing steps for a single image (e.g. atmospheric, radiometric, geometric correction) are carried out automatically, thus making these data readily available in the aftermath of a natural or man-made event threatening a cultural heritage site.

The usual way of assessing damages is change detection, in which a pre-event image available in the archive is compared by image analysts to a new acquisition. Such process is often carried out by visual analysis (Plank et al. 2015), decreasing the timeliness in production and sometimes the completeness of a damage assessment or risk estimation map. It would therefore be desirable to increase the automation

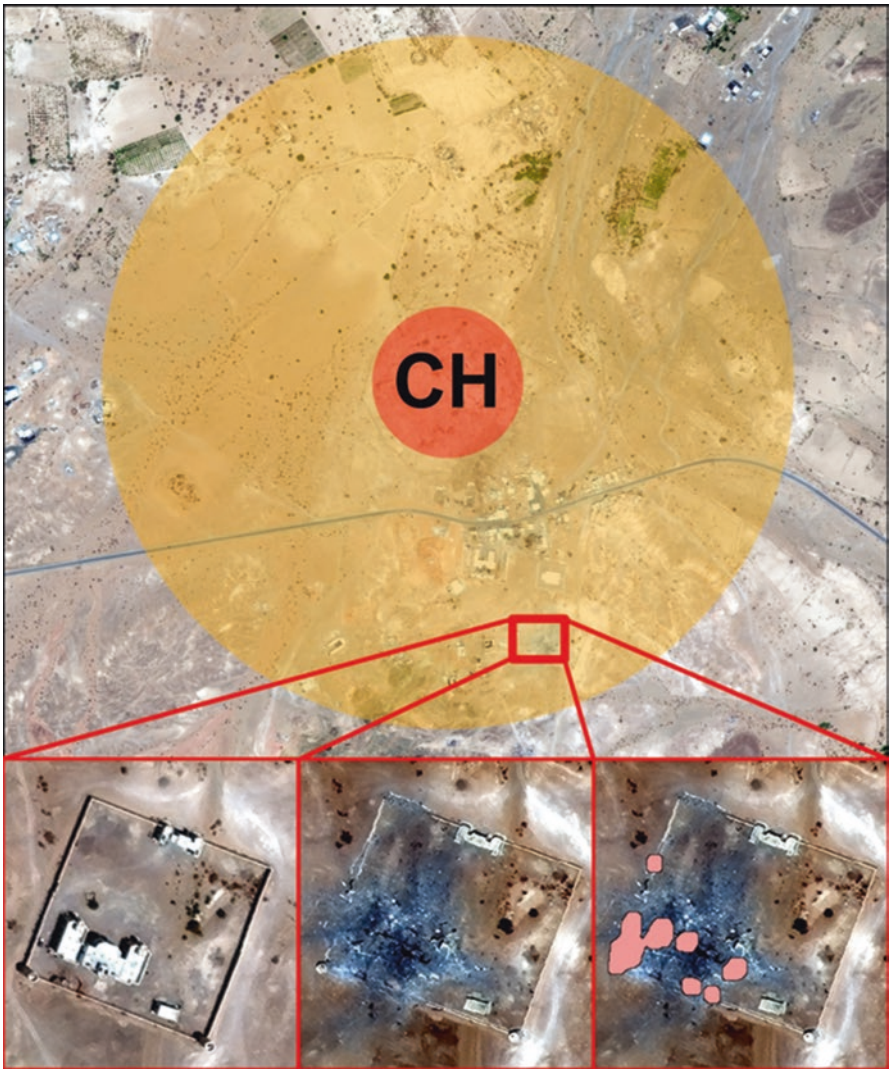

Fig. 14 Top: Possible definition of high-sensitivity (red) and medium-sensitivity (yellow) areas in Sirwah. Bottom: change detection analysis based on Gabor features of a building in the medium-sensitivity area; from left to right, image acquired before the event, image acquired after the event and change detection results

degree of such response (Lasaponara and Masini 2012). This chapter illustrates the use of absolute differences in Gabor texture features in order to derive robust change maps, which can provide image analysts with a valuable input to speed up their anyway necessary verification of the entity of damages in a sensitive area.

The case of study of Palmyra in Syria, which became unfortunately well-known for the recent destruction to its cultural heritage carried out by the so-called

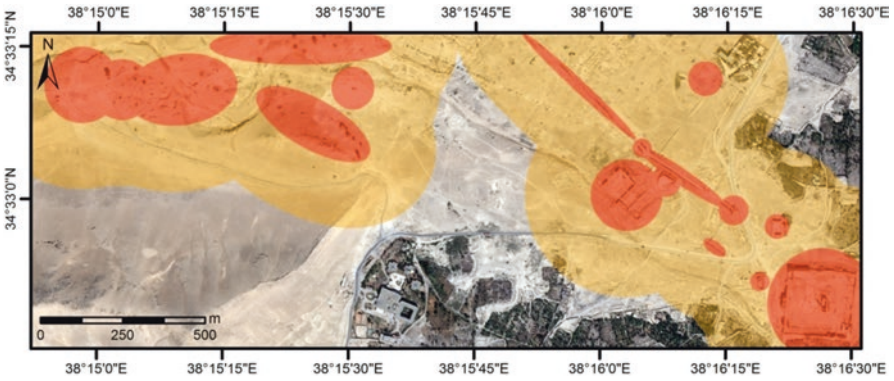

Fig. 15 Possible definition of high- and medium-sensitivity areas in Palmyra: high priority zones rich in CH sites are represented in red, while surrounding areas which could be monitored during critical events are marked in yellow

Islamic state, is analysed to demonstrate the capabilities of such computer-aided system. A reference map verified by authorities reporting all sites which suffered damages in the last years is used as ground truth: this is almost identical to the results of the described change detection algorithm.

The analysis of the most useful Gabor features employed suggests that more reliable change detection maps could be achieved by preselecting the orientation of texture filters as a function of image resolution and of the sun's position, if the images are acquired by the same heliosynchronous satellite.

In order to have a complete overview on the damaged sites, an older auxiliary image acquired over Palmyra is extracted from Google Earth. This has two positive aspects: firstly, it shows that expensive archive data could be replaced by more easily available data sources; secondly, it enables a multi-temporal representation of the evolution for damage extent over time.

In 2017, further destruction to Palmyra's cultural sites has been reported (Danti et al. 2017). With the aid of two recent acquisitions, this additional damage has been assessed, and a more complete map reporting the chronological sequence of the attacks is derived.

The described methodology could be applied in such inaccessible areas affected by natural or anthropogenic hazards, until in situ investigations can be performed. The general planning related to the development of risk-preparedness strategies for CH sites could therefore benefit from the derived change maps, contributing to the effectiveness of rapid response strategies in case of disasters. Ideally, if World Heritage site VHR data for non-accessible sites would become easily available, an automatic change map could raise an alarm only minutes after the acquisition of a new image of the area. This should be later verified by experts—first, by visual analysis of the data and, subsequently, by information sources in situ. Projects aiming at integrating earth observation in cultural heritage monitoring processes in a solid framework could benefit from employing such a workflow (GEO 2016; CIP 2016).

Envisaging a possible frame for machine-assisted damage assessment in sensitive sites, the advantages for a user of being able to define areas with different priority are discussed. We analyse the case of civil unrest in Sirwah, Yemen, in which cultural sites have not been reported as damaged, but some surrounding buildings have been destroyed. In case of critical events, it may be relevant to expand the area of interest for the damage detection routine, as the destruction of surrounding buildings may indicate a threat to the cultural sites.

Future work should include an evaluation of the results for additional test sites in different time frames and geographical areas, while false alarms could be decreased by restricting the analysis to high priority areas comprising relevant CH sites only.

Acknowledgements The authors would like to thank Jiaojiao Tian (German Aerospace Center-DLR) and Vasiliki Lysandrou (Cyprus University of Technology-CUT) for their valuable inputs contained in the paper (Cerra et al. 2016), which was the starting point for the preparation of this book chapter.

References

Agapiou A, Hadjimitsis DG, Alexakis DD (2013) Development of an image-based method for the detection of archaeological buried relics using multi-temporal satellite imagery. Int J Remote Sens 34:5979–5996

Agapiou A, Lysandrou V, Themistocleous K, Hadjimitsis D (2016) Risk assessment of cultural heritage sites clusters using satellite imagery and GIS: the case study of Paphos District. Cyprus Nat Hazards:1–16. https://doi.org/10.1007/s11069-016-2211-6

Aguilar M, del Mar Saldan˜a M, Aguilar FJ, Fern'andez I (2013) Radiometric comparison between GeoEye-1 and WorldView-2 panchromatic and multispectral imagery. INGEGRAF-ADM-AIP PRIMECA. Ingegraf, Madrid, pp 1–9

Al Masdar News Die Erforschung der sabischen Stadtanlage und Oase von Sirwah (Provinz Marib). Available online: https://www.almasdarnews.com/article/yemeni-ceasefire-expires-clashes-erupt-across-ountry. Accessed on 19 Oct 2017

Bryce TR (2014) Ancient Syria: a three thousand year history. Oxford University Press

Cantineau J (1934) Inventaire des Inscriptions de Palmyre Fasc IX: le Sanctuaire de Bel. Damascus Museum, Damascus, p 8

Casana J, Panahipour M (2014) Satellite-based monitoring of looting and damage to archaeological sites in Syria. J East Mediterr Archaeol Herit Stud 2:128–151

Cerra D, Plank S, Lysandrou V, Tian J (2016) Cultural heritage sites in danger - towards automatic damage detection from space. Remote Sens 8:9

CIPA Heritage Documentation, 2016

Contreras DA (2010) Huaqueros and remote sensing imagery: assessing looting damage in the Vir Valley, Peru. Antiquity 84:544–555

Council of Europe. European Landscape Convention; Report and Convention; Council of Europe: Florence, Italy, 2000

Cuneo A, Penacho S, Gordon LB (2015) Special report: update on the Situation in Palmyra, . Available online: http://www.asor-syrianheritage.org/special-report-update-on-the-situation-in-palmyra. Accessed on 19 Oct 2017

Cunliffe E (2014) Remote assessments of site damage: a new ontology. Int J Herit Digit Era 3:453–473

Danti M (2001) Palmyrene funerary sculptures at Penn. Expedition 43:33–40

Danti M, Cuneo A, Gabriel M, Penacho S New Damage in Palmyra Uncovered by ASOR CHI. Available online: http://www.asor-syrianheritage.org/new-damage-in-palmyra-uncovered-by-asor-chi. Accessed on 19 Oct 2017

Earth Observation in Cultural Heritage Documentation, 2016. Accessed on 19 Sept 2016

Evans D (2016) Airborne laser scanning as a method for exploring long-term socio-ecological dynamics in Cambodia. J Archaeol Sci. https://doi.org/10.1016/j.jas.2016.05.009

Gerlach I Die Erforschung der sabischen Stadtanlage und Oase von Sirwah (Provinz Marib). Available online (in German): https://fallback.dainst.org/projekt/-/project-display/102061. Accessed on 19 Oct 2017

Grigorescu SE, Petkov N, Kruizinga P (2002) Comparison of texture features based on Gabor filters. IEEE Trans Image Process 11:1160–1167

Haghighat M, Zonouz S, Abdel-Mottaleb M (2015) CloudID: trustworthy cloud-based and cross-enterprise biometric identification. Expert Syst Appl 42:7905–7916

Lasaponara R, Masini N (2007) Detection of archaeological crop marks by using satellite QuickBird multispectral imagery. J Archaeol Sci 34:214–221

Lasaponara R, Masini N (2011) Satellite remote sensing in archaeology: past, present and future perspectives. J Archaeol Sci 38:1995–2002

Lasaponara R, Masini N (2012) Remote sensing in archaeology: from visual data interpretation to digital data manipulation. Satellite remote sensing: a new tool for archaeology, vol 16. Springer, p 3

Lowe DG (2004) Distinctive image features from scale-invariant Keypoints. Int J Comput Vis 60:91–110

Manjunath BS, Ma WY (1996) Texture features for browsing and retrieval of image data. IEEE Trans Pattern Anal Mach Intell 18:837–842

Plank S, Strunz G, van Ess M, Richardson P (October 2015) Monitoring of cultural heritage sites using VHR earth observation data. Proceedings of the WorldView global Alliance—user conference, Munich, Germany, 13–14

Ramakrishnan AG, Raja SK, Ram HVR (6 September 2002) Neural network-based segmentation of textures using Gabor features. Proceedings of the 12th IEEE Workshop on Neural Networks for Signal Processing, Martigny, pp 365–374

Schuetter J, Goel P, McCorriston J, Park J, Senn M, Harrower M (2013) Autodetection of ancient Arabian tombs in high-resolution satellite imagery. Int J Remote Sens 34:6611–6635

Starcky J, Munajjed S (1960) Palmyra: the Bride of the desert. Directorate-General of Information (Syria), Damascus

Tian J, Cui S, Reinartz P (2014) Building change detection based on satellite stereo imagery and digital surface models. IEEE Trans Geosci Remote Sens 52:406–417

Trier ØD, Larsen SØ, Solberg R (2009) Automatic detection of circular structures in high-resolution satellite images of agricultural land. Archaeol Prospect 16:1–15

Vijayaraj V, Bright EA, Bhaduri BL (2008) Rapid damage assessment from high resolution imagery. Proceedings of the IEEE international geoscience and remote sensing symposium (IGARSS), vol 3, Boston, pp 499–502